ELSEVIER

Journal of Biomechanics 32 (1999) 409–415

JOURNAL OF BIOMECHANICS

A theoretical analysis of preferred pedaling rate selection in endurance cycling

R.R. Neptune[a,*], M.L. Hull[b]

[a]Human Performance Laboratory, Faculty of Kinesiology, University of Calgary, Calgary, AB T2N 1N4, Canada
[b]Department of Mechanical Engineering, University of California, Davis, CA 95616, USA

Received 8 July 1998; accepted 23 November 1998

Abstract

One objective of this study was to investigate whether neuromuscular quantities were associated with preferred pedaling rate selection during submaximal steady-state cycling from a theoretical perspective using a musculoskeletal model with an optimal control analysis. Specific neuromuscular quantities of interest were the individual muscle activation, force, stress and endurance. To achieve this objective, a forward dynamic model of cycling and optimization framework were used to simulate pedaling at three different rates of 75, 90 and 105 rpm at 265 W. The pedaling simulations were produced by optimizing the individual muscle excitation timing and magnitude to reproduce experimentally collected data. The results from these pedaling simulations indicated that all neuromuscular quantities were minimized at 90 rpm when summed across muscles. In the context of endurance cycling, these results suggest that minimizing neuromuscular fatigue is an important mechanism in pedaling rate selection. A second objective was to determine whether any of these quantities could be used to predict the preferred pedaling rate. By using the quantities with the strongest quadratic trends as the performance criterion to be minimized in an optimal control analysis, these quantities were analyzed to assess whether they could be further minimized at 90 rpm and produce normal pedaling mechanics. The results showed that both the integrated muscle activation and average endurance summed across all muscles could be further minimized at 90 rpm indicating that these quantities cannot be used individually to predict preferred pedaling rates.

Keywords: Muscle force; Activation; Neuromuscular quantities; Forward dynamic simulation; Preferred pedaling rate

1. Introduction

There has been considerable research illustrating the discrepancy between pedaling rates that elicit the lowest oxygen demand and the pedaling rates preferred by experienced cyclists. Previous studies have shown that the most economical pedaling rate which minimizes oxygen consumption is between 50 and 65 rpm (e.g. Coast and Welch, 1985; Seabury et al., 1977) while several other studies have shown that cyclists naturally select pedaling rates between 85 and 95 rpm (e.g. Hagberg et al., 1981; Marsh and Martin, 1993). Naturally selected pedaling rates are also called preferred pedaling rates.

This discrepancy has led to experimental studies investigating possible factors associated with preferred pedaling rate selection other than oxygen consumption. Marsh and Martin (1995) examined the individual muscle integrated electromyograms (iEMG) across pedaling rates from 50 to 110 rpm and reported no correlation between iEMG and pedaling rate. But the recent results of Neptune et al. (1997) suggest that minimizing iEMG may be potentially important. They tested competitive cyclists across pedaling rates from 45 to 120 rpm and found that several subjects exhibited a minimum summed iEMG across all muscles tested at 90 rpm. The differences between these studies are possibly related to the methodology used in each study. Although methodological variations make it difficult to reconcile differences in the results, the results of Neptune et al. (1997) suggest that a theoretical analysis of the individual muscle iEMG is warranted.

Previous theoretical studies of pedaling rates have used muscle stress (Hull et al., 1988) and muscle endurance (Hull and Gonzalez, 1988) based cost functions to predict optimal pedaling rates of 100 rpm and

*Corresponding author. Present address: Rehabilitation R & D Center (153), VA Palo Alto Health Care System, 3801 Miranda Avenue, Palo Alto, CA 94304 USA. E-mail: neptune@roses.stanford.edu.

0021-9290/99/$ – see front matter
PII: S0021-9290(98)00182-1

95–100 rpm, respectively. Although these theoretical studies were successful in predicting pedaling rates near the preferred rates of cyclists, these analyses were performed using intersegmental moments computed through inverse dynamics. Although analyses using intersegmental moments provide little insight into how individual muscle mechanics and energetics influence pedaling rate selection, nevertheless, these previous theoretical studies certainly suggest that individual muscle stress and endurance may play an important role in pedaling rate selection.

In contrast to the above experimental studies, musculoskeletal modeling combined with optimal control analysis has recently proven to be a powerful method to study multi-joint movements with respect to individual muscle mechanics and energetics (e.g. Pandy et al., 1995; Raasch et al., 1997). This type of analysis provides considerable information regarding individual muscle kinetics, kinematics and coordination strategies to achieve a given motor task. Optimal control theory has also been applied to forward dynamic simulation studies of cycling to theoretically examine coordination of the lower extremity muscles (e.g. Raasch et al., 1997, Neptune and van den Bogert, 1998). This type of analysis would be a powerful tool to investigate quantities associated with pedaling rate selection because of the vast amount of information available to the researcher at the individual muscle level.

Therefore, the objectives of this study were twofold. One objective was to identify any association between the individual muscle activation, force, stress and endurance quantities and preferred pedaling rate selection using a forward dynamic simulation approach. The identification of muscular quantities that are minimized near 90 rpm may provide important physiological information regarding the mechanisms behind pedaling rate selection. For the quantity(s) found to have the strongest trend (i.e. minimum at 90 rpm and steepest parabolic curve), a second objective was to determine whether observed pedaling mechanics are consistent with the nervous system minimizing that quantity(s). This second objective would indicate whether the quantity could be used to predict the preferred pedaling rate and may have important implications for understanding general movement control principles during other motor tasks.

2. Methods

2.1. Bicycle-rider model

A planar two-legged bicycle–rider model was developed in a previous study (Neptune and Hull, 1998) using SIMM (MusculoGraphics, Inc., Evanston, IL.) and will be briefly reviewed here. Each leg consisted of three rigid-body segments (thigh, shank and foot) with the hip joint center fixed and the foot rigidly attached to the pedal. The model was driven by 14 individual musculotendon actuators that were combined into nine muscles groups, with muscles within each group receiving the same excitation signal. The muscle excitations were modeled as block patterns defined by duration and magnitude and the musculoskeletal geometry and parameters were based on the SIMM model (Delp et al., 1990). The crankload dynamics were modeled by an equivalent inertial and resistive torque applied about the center of the crankarm (Fregly, 1993).

The dynamical equations-of-motion for the bicycle–rider system were derived using SD/FAST (Symbolic Dynamics, Inc., Mountain View, CA) and a forward dynamic simulation was produced by Dynamics Pipeline (MusculoGraphics, Inc., Evanston, IL.). The equations of motion are presented in matrix form as

$$\mathbf{M}(\mathbf{q})\ddot{\mathbf{q}} = \mathbf{V}(\mathbf{q},\dot{\mathbf{q}}) + \mathbf{G}(\mathbf{q}) + \mathbf{D}^{\mathrm{m}}\mathbf{F}^{\mathrm{m}}(\mathbf{q},\dot{\mathbf{q}},\mathbf{a}^{\mathrm{m}},\mathbf{l}^{\mathrm{m}}) + \mathbf{T}(\mathbf{q},\dot{\mathbf{q}}), \tag{1}$$

where $\mathbf{q}$ is the generalized coordinates, $\mathbf{M}(\mathbf{q})$ the system mass matrix, $\mathbf{V}(\mathbf{q},\dot{\mathbf{q}})$ the coriolis and centripetal effects, $\mathbf{G}(\mathbf{q})$ the gravitational terms, $\mathbf{D}^{\mathrm{m}}$ the muscle moment arm matrix, $\mathbf{F}^{\mathrm{m}}(\mathbf{q},\dot{\mathbf{q}},\mathbf{a}^{\mathrm{m}},\mathbf{l}^{\mathrm{m}})$ the musculotendon actuator forces, $\mathbf{a}^{\mathrm{m}}$ the muscle activations, $\mathbf{l}^{\mathrm{m}}$ the muscle lengths and $\mathbf{T}(\mathbf{q},\dot{\mathbf{q}})$ the friction terms.

The force generating capacity of each muscle was based on a generic Hill-type model governed by the muscles' force–length–velocity characteristics (Zajac, 1989) with passive damping added to the force–velocity relationship to make it invertible (Schutte et al., 1993).

The neural excitation ($\mathbf{u}^{\mathrm{m}}$) was coupled to the muscle activation ($\mathbf{a}^{\mathrm{m}}$) through a first-order differential equation (Raasch et al., 1997), with activation and deactivation time constants of 50 and 65 ms, respectively (Winters and Stark, 1988), as

$$\dot{\mathbf{a}}^{\mathrm{m}} = \begin{cases} (\mathbf{u}^{\mathrm{m}} - \mathbf{a}^{\mathrm{m}})\cdot(c_1\mathbf{u}^{\mathrm{m}} + [c_2 \cdots c_2]^{\mathrm{T}}) & \mathbf{u}^{\mathrm{m}} \geqslant \mathbf{a}^{\mathrm{m}}, \\ (\mathbf{u}^{\mathrm{m}} - \mathbf{a}^{\mathrm{m}})\cdot c_2 & \mathbf{u}^{\mathrm{m}} < \mathbf{a}^{\mathrm{m}}, \end{cases} \tag{2}$$

where c_1 and c_2 are functions of the activation and deactivation time constants with $c_1 = \tau_{\mathrm{act}}^{-1} - \tau_{\mathrm{deact}}^{-1}$ and $c_2 = \tau_{\mathrm{deact}}^{-1}$.

The performance criterion used in the optimization to find the optimal muscle control vector ($\mathbf{u}^{\mathrm{m}}$) was formulated to solve a 'tracking' problem by minimizing the differences between experimental and model crank torque, pedal force, intersegmental hip, knee, and ankle joint moment, and muscle excitation onset and offset timing data. The 'experimental' intersegmental moment data were derived from inverse dynamics computations that used the experimental kinematic and pedal force data as input. This criterion was shown in a previous

study to produce a pedaling simulation that reproduces experimental pedaling data (Neptune and Hull, 1998). Specifically, the performance criterion was the sum of squared residuals normalized by the inter-subject variability in the form of:

$$J = \sum_{j=1}^{m} \sum_{i=1}^{n} \frac{(Y_{ij} - \hat{Y}_{ij})^2}{\mathrm{SD}_{ij}^2} + \sum_{k=1}^{n_{\mathrm{mus}}} \sum_{l=1}^{2} \frac{(E_{kl} - \hat{E}_{kl})}{\mathrm{SD}_{kl}^2}, \quad (3)$$

where Y_{ij} is the experimental kinematic and kinetic data, $\hat{Y}_{ij}$ the simulation data corresponding to Y_{ij}, SD_{ij} the inter-subject standard deviation, n the number of time steps, m the number of kinematic and kinetic tracking quantities evaluated, E_{kl} the experimental onset and offset timing of muscle k, $\hat{E}_{kl}$ the simulation data corresponding to E_{kl}, and n_{mus} the number of muscle groups ($n_{\mathrm{mus}} = 9$).

A simulated annealing algorithm (Goffe et al., 1994) was used to find the individual muscle excitation onset, offset and magnitude which minimized the performance criterion (Eq. (3)) over the time interval $[0, t_{\mathrm{final}}]$, where t_{final} was determined by the pedaling rate simulated (75, 90 or 105 rpm, respectively). Simulations were performed over four revolutions to assure that initial start-up transients had decayed and the simulation had reached steady state. Final time constraints were enforced during the fourth revolution to ensure that the model pedaled at the required average pedaling rate and power output of 265 W.

A total of nine quantities was computed for each muscle, at each of the simulated pedaling rates, for evaluation of importance to the preferred pedaling rate. Three of these quantities were derived from the muscle activation and included the mean and peak activation as well as the integrated muscle activation (iACT). The iACT was computed within the model excitation onset and offset angles and normalized to the time per cycle for each muscle. The remaining six quantities were all based on the muscle force and included both the mean and peak of the muscle force, the muscle stress and the endurance. Muscle stress was computed as

$$\mathbf{stress} = \frac{\mathbf{F}^{\mathrm{m}}}{PCSA^{\mathrm{m}}} \quad (4)$$

where $\mathbf{F}^{\mathrm{m}}$ is the individual muscle force, and $PCSA^{\mathrm{m}}$ is the muscle physiologic cross-sectional area.

PCSA values were computed by normalizing each muscle's maximum isometric force by a maximum muscle stress of $0.8\ \mathrm{MN/m^2}$, and muscle endurance was estimated as (Crowninshield and Brand, 1981):

$$\mathbf{endurance} = \left(\frac{\mathbf{F}^{\mathrm{m}}}{PCSA^{\mathrm{m}}}\right)^2. \quad (5)$$

All mean quantities were computed as the average value over the crank cycle. Each quantity was examined at the individual muscle level and then summed across all muscles to assess whether the sum was minimized at 90 rpm. Since more than one quantity was minimized at 90 rpm, each quantity at all three pedaling rates was normalized to the value of that quantity at 90 rpm and then the normalized values at 75 and 105 rpm were compared across all quantities to determine which quantity(s) had the strongest quadratic trend.

To determine whether any quantities minimized at 90 rpm (i.e. preferred pedaling rate) could be used to predict this pedaling rate, the forward dynamic model and optimization framework described above were used. The only difference was the performance criterion used in the optimization. Rather than minimizing the RMS errors between the simulation and experimental data, the criterion minimized the quantity(s) that was identified as having the strongest quadratic trend.

2.2. Experimental data

To provide data for the tracking problem, both kinetic and kinematic data were collected from 11 male competitive cyclists (avg. and std. dev. of height $= 1.79 \pm 0.07$ m; weight $= 68.8 \pm 7.6$ kg; age $= 22.2 \pm 2.7$ yr). Informed consent was obtained before the experiment. The subjects rode a conventional racing bicycle mounted on an electronically braked Schwinn Velodyne ergometer. The protocol consisted of a 15-min warm-up period at a workrate of 150 W at 90 rpm. Then, each subject cycled at a workrate of 265 W at three different pedaling rates (75, 90 and 105 rpm) randomly assigned to control for possible interactions and fatigue. After a 3-minute adaptation period, data collection was randomly initiated twice during the following 2 min for 10 s each.

The intersegmental moments were computed using a standard inverse dynamics approach. The rider was modeled as a five-bar linkage in plane motion. The equations of motion for each link were solved using inverse dynamics, starting with the foot and proceeding through each link to the hip. The anthropometric estimates of each segment's mass and center of gravity were defined based on the work of Dempster (1955). Moments of inertia were computed by the data presented in Whittsett (1963) which were personalized to each subject based on the work of Dapena (1978).

The necessary kinematic data were recorded using a combination of video-based motion analysis and direct measurement. The intersegmental joint centers were obtained using a high-speed video system (Motion Analysis Corp., Santa Rosa, CA) from reflective markers located over the right anterior–superior iliac spine (ASIS), greater trochanter, lateral epicondyle, lateral malleolus, pedal spindle and crank spindle. The hip joint center was located relative to the marker over the ASIS based on the methodology presented in Neptune and Hull (1995). Angular orientation data of the crank arm and pedal

were collected simultaneously with two optical encoders sampled at 100 Hz. Both the video and encoder data were filtered using a fourth-order zero phase shift Butterworth low pass filter with a cutoff frequency of 9 Hz. All derivatives to determine coordinate velocity and acceleration were calculated by fitting a quintic spline to the position data and differentiating the resulting equations.

The pedal force data were collected simultaneously with the video and encoder data using the pedal dynamometer described by Newmiller et al. (1988). The pedal force data were filtered using a fourth-order zero phase shift Butterworth low pass filter with a cutoff frequency of 20 Hz. The filtered pedal force and encoder data were linearly interpolated to correspond in time with the video coordinate data.

Electromyographic (EMG) data collected in Neptune et al. (1997) under similar pedaling conditions provided the muscle timing defined by EMG onset and offset to evaluate the excitation timing error in Eq. (3). The reader is referred to that text for details on the data collection and processing. The EMG timing data for the hamstring muscle group (HAMS) were used to compute the excitation timing error for both the biceps femoris short head muscle (BFsh) and HAMS in the model. No experimental EMG data were available for the PSOAS muscle so it was not included in the excitation error calculation.

The tracking quantities were computed on a cycle-by-cycle basis, averaged across cycles for each subject and then averaged across subjects.

3. Results

The simulation results showed that all nine quantities were minimized at the 90 rpm pedaling rate (Fig. 1). Examination of the individual muscle activation quantities revealed that only the average VAS and peak GAS muscle activations were not minimized at 90 rpm (Table 1). When the individual muscle activation quantities were summed across all muscles, the minimum value always occurred at the 90 rpm pedaling rate (Fig. 1).

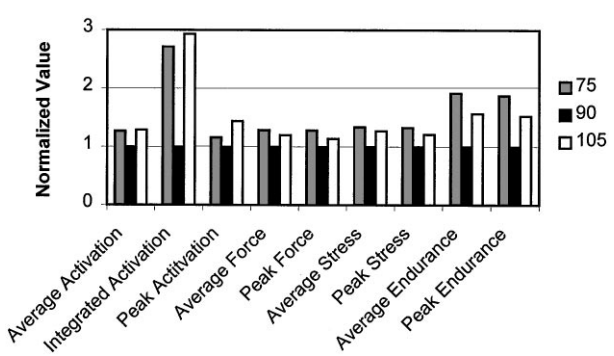

Fig. 1. Summary of the normalized neuromuscular quantities across the different pedaling rates.

Table 1
The average muscle activation over the crank cycle for each of the three pedaling rates. The summed values are across all muscles. The last row is the summed data normalized to the lowest value. The 14 muscles included in the model were the soleus (SOL), gastrocnemius (GAS), medial hamstrings (HAMS), biceps femoris short (BFsh), psoas (PSOAS), tibialis anterior (TA), rectus femoris (RF), 3-part vastus (VAS1, VAS2 and VAS3), gluteus maximus (GMAX), biceps femoris long (BF), iliacus (IL) and adductor magnus (ADMAG)

	Average muscle activation		
Muscle	[**75**]	[**90**]	[**105**]
SOL	0.23	0.21	0.31
GAS	0.32	0.31	0.53
HAMS	0.42	0.34	0.46
BFsh	0.66	0.35	0.62
PSOAS	0.66	0.51	0.6
TA	0.33	0.27	0.4
RF	0.31	0.28	0.34
VASI	0.33	0.24	0.23
GMAX	0.42	0.37	0.45
BFlg	0.42	0.34	0.46
IL	0.66	0.51	0.6
VAS2	0.33	0.24	0.23
VAS3	0.33	0.24	0.23
ADMAG	0.42	0.37	0.45
Sum	5.84	**4.58**	5.91
Normalized	1.27	**1.00**	1.29

Similar to the individual muscle activations, the muscle force quantities were generally minimized at the 90 rpm pedaling rate. Although not presented in detail, the average muscle force displayed the strongest tendency to be minimized at 90 rpm with 12 out of the 14 minimum average muscle forces occurring at 90 rpm. The peak muscle force also displayed a strong tendency to be minimized at 90 rpm, with minimum values occurring at 90 rpm in 9 out of the 14 muscles. For both muscle force quantities, the summed value across all muscles was clearly a minimum at 90 rpm (Fig. 1). The trends for the average and peak muscle stress and endurance quantities were also similar to the muscle activation and muscle force quantities with minimums occurring at the 90 rpm pedaling rate (Fig. 1).

Because the summed integrated muscle activation and average endurance quantities displayed the strongest quadratic trends to be minimized at 90 rpm (Fig. 1), these quantities were used in the verification optimization to determine whether they were absolutely minimized at 90 rpm. When these quantities were used as the performance criterion to determine the muscle stimulation patterns, the results revealed that neither of these quantities was absolutely minimized at 90 rpm. In addition, the pedaling mechanics were quite different from those generated from Eq. (3). Although the average pedaling rate constraint of 90 rpm was satisfied, the pedaling

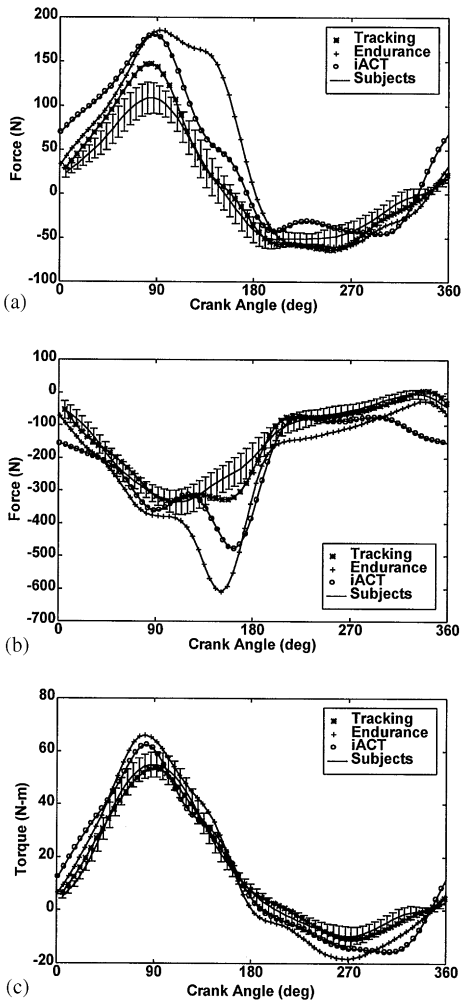

Fig. 2. Comparison of simulation pedaling mechanics for the tracking, integrated activation, and average endurance performance criteria against the results derived experimentally from a subject sample: (a) horizontal pedal force over the crank cycle, (b) vertical pedal force, and (c) crank torque. The crank angle is 0° at top-dead-center and positive in the clockwise direction. The error bars indicate ±1 standard deviation.

mechanics (horizontal and vertical pedal forces and crank torque) to perform this task were quite different (Fig. 2).

4. Discussion

The goals of this study were to determine whether muscle activation, force, stress and endurance quantities were associated with preferred pedaling rate selection from a theoretical perspective and also to verify whether any of these quantities could be used to predict the preferred pedaling rate. To achieve these goals, a forward dynamic simulation of cycling and optimization framework developed in a previous study (Neptune and Hull, 1998) were used to quantify the various neuromuscular quantities at pedaling rates of 75, 90 and 105 rpm at 265 W and to verify whether these quantities were absolutely minimized.

Before the results are discussed in light of the above stated goals, discussion regarding some of the methodological issues is warranted. One issue concerns the validity of the simulations. The pedal and crank kinetic and kinematic quantities were previously shown to match closely with experimental data when using the performance criterion in Eq. (3) at 90 rpm (Neptune and Hull, 1998). Although the kinetic and kinematic quantities for the other pedaling rates were not presented in the present study, the RMS errors were consistent across pedaling rates and comparable in magnitude with the 90 rpm data. Further, the muscle activation timing was consistent with experimental data collected in Neptune et al. (1997) during similar pedaling conditions as the present study.

A second methodological issue concerns the choice of the computed quantities. Because three of the nine quantities computed were derived from the average muscle force (i.e. average muscle force, stress and endurance) and an additional three from the peak muscle force (i.e. peak muscle force, stress and endurance), the quantities in these two groups of three were related to some degree. However, the summed quantities in each group were not directly related to the corresponding muscle force quantity because of the additional mathematical operation to derive the stress and endurance quantities and also the subsequent summing operation. Accordingly, the strengths of the quadratic trends for the quantities in each group were different (Fig. 1). Considering that the quantities to be used in the second optimization were selected based on the strength of the quadratic trend, the use of related quantities in the analysis was justified.

With both the validity of the simulation results and the propriety of the computed quantities established, it is useful to discuss the results in the context of preferred pedaling rate selection. Examination of the average individual muscle activation, force, stress and endurance quantities showed that the minimum values occurred primarily at the 90 rpm pedaling rate with the summed minimum values occurring always at 90 rpm (Fig. 1). These results suggest that in endurance cycling, minimizing neuromuscular fatigue-related quantities is a contributing mechanism in pedaling rate selection. This hypothesis has been previously suggested in experimental studies examining the electromyogram (e.g. Takaishi et al., 1994) and intersegmental joint moments (e.g. Hull et al., 1988), and now is further supported by the results of this study examining individual neuromuscular quantities.

The natural selection of higher pedaling rates over the more metabolically efficient lower pedaling rates has been linked to the linear relationship between pedaling rate and the required pedaling torque during constant

average power output cycling (e.g. Takaishi et al., 1994). Theoretically, to maintain constant average power output, as pedaling rate increases, the required pedaling torque decreases, and thus the required muscular forces should also decrease. This relationship led Takaishi et al. (1994) to speculate that cyclists prefer higher pedaling rates to minimize neuromuscular fatigue. But the results of the present study have shown that this hypothesis is only valid up to 90 rpm, after which the muscular forces begin to increase again. Evidence suggests that the increases in muscular forces are related to the crank cycle duration. As pedaling rate increases, the time duration per cycle decreases. Therefore, the muscle force magnitude appears to increase during the shorter time duration in order to satisfy the pedaling torque requirements. Thus, at both lower and higher pedaling rates, the muscular force requirements are higher than those at 90 rpm indicating that the pedaling rate naturally selected by cyclists is the optimal pedaling rate to minimize muscle force and neuromuscular fatigue.

The results of this study are also consistent with muscle fiber recruitment and metabolism theories. As mentioned in the Results section but not presented in detail, the 90 rpm pedaling rate had the lowest peak muscle forces in 9 of 14 muscles modeled. Recent work in cycling has supported the premise that muscle fibers are recruited based on the force requirements of the task with fast twitch fibers being recruited for the higher force requirements (Ahlquist et al., 1992). The lower muscle force requirements at 90 rpm allow for a larger percentage of active slow-twitch muscle fibers which have higher mechanical efficiency (Coyle et al., 1992) and avoid the lactate buildup associated with fast twitch fiber metabolism and neuromuscular fatigue (e.g. Coyle et al., 1991).

Similar to inverse dynamics-based analyses, an implicit assumption in the optimal tracking solution in the present study was that the muscle controls that minimized the tracking errors and produced quadratic trends of each quantity, were produced as a result of the nervous system minimizing the corresponding neuromuscular quantity. But unlike inverse dynamics-based analyses, we can explicitly test this assumption with a subsequent optimization using the quantity itself as the performance criterion to be minimized. If the results from this optimization showed that the quantity was absolutely minimized at 90 rpm in the tracking problem, and that the corresponding pedaling mechanics were representative of those experimentally determined at the preferred pedaling rate, then this would indicate that the quantity could be used to predict the preferred pedaling rate and may have important implications for understanding general movement control principles during other motor tasks.

The verification analysis of the integrated muscle activation and the average endurance quantities found that the optimization further reduced these quantities at 90 rpm beyond the minimum value obtained in the tracking problem, and also that the changes in pedaling mechanics (horizontal and vertical pedal forces) were substantial (Fig. 2). Therefore, it is evident that these neuromuscular quantities are not the only determinants in pedaling rate selection.

An underlying goal of this study was to identify a performance measure (i.e. neuromuscular quantity) that could be used within a forward dynamic optimization framework to identify equipment setup to optimize performance. Assuming that performance is optimized at a cyclist's preferred pedaling rate, performance can be increased by determining equipment that minimizes the performance criterion that predicts a cyclist's preferred pedaling rate. But the results of this study showed that the identification of a measure based upon a single neuromuscular quantity to be used in an optimization framework that will predict preferred pedaling rates might be difficult. Many neuromuscular quantities were shown here to be associated with pedaling rate selection so that the correct combination and weighting of these quantities in a single measure may be difficult to achieve.

Acknowledgements

This research was made possible through the financial support of Shimano Corporation of Osaka, Japan and specifically Shinpei Okajima and Wayne Stetina. The authors are also grateful to Dr. Steve Kautz for his valuable contributions throughout this project.

References

Ahlquist, L.E., Bassett Jr, D.R., Sufit, R., Nagle, F.J., Thomas, D.P., 1992. The effect of pedaling frequency on glycogen depletion rates in type I and type II quadriceps muscle fibers during submaximal cycling exercise. European Journal of Applied Physiology 65, 360–364.

Coast, J.R., Welch, H.G., 1985. Linear increase in optimal pedal rate with increased power output in cycle ergometry. European Journal of Applied Physiology 53, 339–342.

Coyle, E.F., Feltner, M.E., Kautz, S.A., Hamilton, M.T., Montain, S.J., Baylor, A.M., Abraham, L.D., Petrek, G.W., 1991. Physiological and biomechanical factors associated with elite endurance cycling performance. Medical Science in Sports Exercise 23, 93–107.

Coyle, E.F., Sidossis, L.S., Horowitz, J.F., Beltz, J.D., 1992. Cycling efficiency is related to the percentage of type I muscle fibers. Medical Science in Sports Exercise 24, 782–788.

Crowninshield, R.D., Brand, R.A., 1981. A physiologically based criterion of muscle force prediction in locomotion. Journal of Biomechanics 14, 793–801.

Dapena, J., 1978. A method to determine the angular momentum of a human body about three orthogonal axes passing through its center of gravity. Journal of Biomechanics 11, 251–256.

Delp, S.L., Loan, J.P., Hoy, M.G., Zajac, F.E., Topp, E.L., Rosen, J.M., 1990. An interactive graphics-based model of the lower extremity to study orthopaedic surgical procedures. IEEE Transactions of Biomedical Engineering 37, 757–767.

Dempster, W. T., 1955. Space requirements of the seated operator. WADC Technical Report 55–159. Wright-Patterson Air Force Base, Dayton, OH.

Fregly, B. J., 1993. The significance of crank load dynamics to steady-state pedaling biomechanics: an experimental and computer modeling study. Ph.D. Dissertation, Stanford University, Stanford, CA.

Goffe, W.L., Ferrier, G.D., Rogers, J., 1994. Global optimization of statistical functions with simulated annealing. Journal of Econometrics 60, 65–99.

Hagberg, J.M., Mullin, J.P., Giese, M.D., Spitznagel, E., 1981. Effect of pedaling rate on submaximal exercise responses of competitive cyclists. Journal of Applied Physiology 51, 447–451.

Hull, M.L., Gonzalez, H.K., Redfield, R., 1988. Optimization of pedaling rate in cycling using a muscle stress-based objective function. International Journal of Sports Biomechanics 4, 1–20.

Hull, M.L., Gonzalez, H., 1988. Bivariate optimization of pedalling rate and crank arm length in cycling. Journal of Biomechanics 21, 839–849.

Marsh, A.P., Martin, P.E., 1993. The association between cycling experience and preferred and most economical cadences. Medical Science in Sports Exercise 25, 1269–1274.

Marsh, A.P., Martin, P.E., 1995. The relationship between cadence and lower extremity EMG in cyclists and noncyclists. Medical Science Sports Exercise 27, 217–225.

Neptune, R.R., Kautz, S.A., Hull, M.L., 1997. The effect of pedaling rate on coordination in cycling. Journal of Biomechanics 30, 1051–1058.

Neptune, R.R., Hull, M.L., 1995. Accuracy assessment of methods for determining hip movement in seated cycling. Journal of Biomechanics 28, 423–437.

Neptune, R.R., Hull, M.L., 1998. Evaluation of performance criteria for simulation of submaximal steady-state cycling using a forward dynamic model. Journal of Biomechanics Engineering 120, 334–341.

Neptune, R.R., van den Bogert, A.J., 1998. Standard mechanical energy analyses do not correlate with muscle work in cycling. Journal of Biomechanics 31, 239–245.

Newmiller, J., Hull, M.L., Zajac, F.E., 1988. A mechanically decoupled two force component bicycle pedal dynamometer. Journal of Biomechanics 21, 375–386.

Pandy, M.G., Garner, B.A., Anderson, F.C., 1995. Optimal control of non-ballistic muscular movements: a constraint-based performance criterion for rising from a chair. Journal of Biomechanical Engineering 117, 15–26.

Raasch, C.C., Zajac, F.E., Ma, B., Levine, W.S., 1997. Muscle coordination of maximum-speed pedaling. Journal of Biomechanics 30, 595–602.

Schutte, L.M., Rodgers, M.M., Zajac, F.E., Glaser, R.M., 1993. Improving the efficacy of electrical stimulation-induced cycle ergometry: an analysis based on dynamic musculoskeletal model. IEEE Transactions of Rehabilitation Engineering 1, 109–125.

Seabury, J.J., Adams, W.C., Ramey, M.R., 1977. Influence of pedalling rate and power output on energy expenditure during bicycle ergometry. Ergonomics 20, 491–498.

Takaishi, T., Yasuda, Y., Moritani, T., 1994. Neuromuscular fatigue during prolonged pedalling exercise at different pedalling rates. European Journal of Applied Physiology 69, 154–158.

Winters, J.M., Stark, L., 1988. Estimated mechanical properties of synergistic muscles involved in movements of a variety of human joints. Journal of Biomechanics 21, 1027–1041.

Zajac, F.E., 1989. Muscle and tendon: properties, models, scaling, and application to biomechanics and motor control. Critical Reviews in Biomedical Engineering 17, 359–411.